

A Small-Molecule FRET Reporter for the Real-Time Visualization of Cell-Surface Proteolytic Enzyme Functions**

Jing Mu, Fang Liu,* Muhammad Shafiq Rajab, Meng Shi, Shuang Li, Chiching Goh, Lei Lu, Qing-Hua Xu, Bin Liu, Lai Guan Ng, and Bengang Xing*

Abstract: Real-time imaging of cell-surface-associated proteolytic enzymes is critical to better understand their performances in both physiological and pathological processes. However, most current approaches are limited by their complexity and poor membrane-anchoring properties. Herein, we have designed and synthesized a unique small-molecule fluorescent probe, which combines the principles of passive exogenous membrane insertion and Förster resonance energy transfer (FRET) to image cell-surface-localized furin-like convertase activities. The membrane-associated furin-like enzymatic cleavage of the peptide probe leads to an increased fluorescence intensity which was mainly localized on the plasma membrane of the furin-expressed cells. This small-molecule fluorescent probe may serve as a unique and reliable reporter for real-time visualization of endogenous cell-surface-associated proteolytic furin-like enzyme functions in live cells and tissues using one-photon and two-photon microscopy.

Cell surface proteolytic enzymes play critical roles in physiological and pathological processes ranging from extracellular matrix processing, growth factors, and the activation of receptors to microbial invasion.^[1] These proteolytic events have not only been implicated in the site-specific cleavage of bioactive proteins or peptide substrates within transmem-

brane domains, thus performing various biological functions, but they are also involved in the progression of various degenerative diseases including cancer, atherosclerosis, and neurological disorder.^[1] Therefore, diagnostic targeting and regulation of proteolysis has become a promising approach to understand the basic pathological pathways and even to treat cancer and other diseases.^[2]

Furin, a membrane-localized proteolytic processing enzyme that belongs to the proprotein convertase (PC) family, is ubiquitously expressed and functions within secretory and endocytic pathways and at the cell surface. Normally, these furin-like convertases can activate a variety of protein precursors in intracellular membrane and cell-surface systems, and process them into biologically functional peptides and proteins.^[3] For example, furin has been established to be involved in the intramembrane processing of several kinds of matrix metalloproteinases (MMPs), which were found to have elevated levels in several types of human cancers.^[4] The activation of α - and β -secretases, two key enzymes in processing the generation of toxic amyloid peptides during the development of Alzheimer's disease (AD), was also found to be mediated by the proteolytic activities of furin.^[5] As well as activities contributing to chronic pathological conditions, cell-surface-associated furin or furin-like proprotein processing is also highly relevant to the maturation of bacterial toxins and the propagation of many non-enveloped or lipid-enveloped viral pathogens, which are prerequisite processes to mediate bacterial or viral invasion into host cells.^[6] Considering the many roles of furin in human pathophysiology, effective strategies to visualize cell-surface-associated furin activities in real-time are therefore rather important. This visualization of cell-surface furin activity will pave the way for elucidating cell-membrane functions and understanding furin-dependent dynamic processes in living cells, thus making them potential targets for the development of new therapeutic agents. Recently, fluorescent biological reporters, such as green fluorescent protein (GFP) or genetically encoded fluorescent protein variants, have been introduced as labels to image extracellular furin activities.^[7] A similar noninvasive investigation of cell-surface proteolytic furin activity was also achieved in single cells based on re-engineered anthrax toxin β -lactamase protein mutants.^[7c] Although all of these approaches were successful in principle, these genetic manipulations may potentially perturb the cell's physiology and cause unexpected biological responses.^[7] In contrast, a small-molecule-based probing technology with desirable properties, such as simple preparation and manipulation, may offer an attractive alternative to compensate for the shortcomings of genetic

[*] J. Mu, Dr. F. Liu, M. S. Rajab, Prof. B. G. Xing
Division of Chemistry and Biological Chemistry
School of Physical & Mathematical Sciences
Nanyang Technological University, Singapore, 637371 (Singapore)
E-mail: Liuf0019@e.ntu.edu.sg
Bengang@ntu.edu.sg

M. Shi, Prof. L. Lu
School of Biological Sciences, Nanyang Technological University
Singapore, 637551 (Singapore)

S. Li, Prof. Q. H. Xu
Department of Chemistry
National University of Singapore, Singapore 117543 (Singapore)

Prof. B. Liu
Department of Chemical Biomolecular Engineering
National University of Singapore, Singapore 117576 (Singapore)

C. Goh, Dr. L. G. Ng
Singapore Immunology Network (SIgN)
A*STAR (Agency for Science, Technology and Research)
Biopolis, Singapore, 138648 (Singapore)

[**] This work was supported by Nanyang Technological University, Singapore through a Start-Up Grant (SUG) RG11/13, RG 64/10 COS research collaboration award. FRET = Förster resonance energy transfer.



Supporting information for this article is available on the WWW under <http://dx.doi.org/10.1002/anie.201407182>.

manipulation.^[8] Unfortunately, because of rapid diffusion and poor immobilizing ability on the cell surface, most established small-molecule fluorescent reporters for furin-like assays (such as the fluorogenic furin convertase substrate Boc-RVRR-AMC) are mainly applied in fixed cells or cell-lysate systems.^[9] The rational design of simple and reliable small-molecule probes with unique tractability and immobilizing properties for real-time imaging of specific cell-membrane-associated furin activity in living cells or tissues is a topic of interest and significance. To our knowledge, such highly specific and activatable cell-surface-anchored reporters have not yet been well exploited.

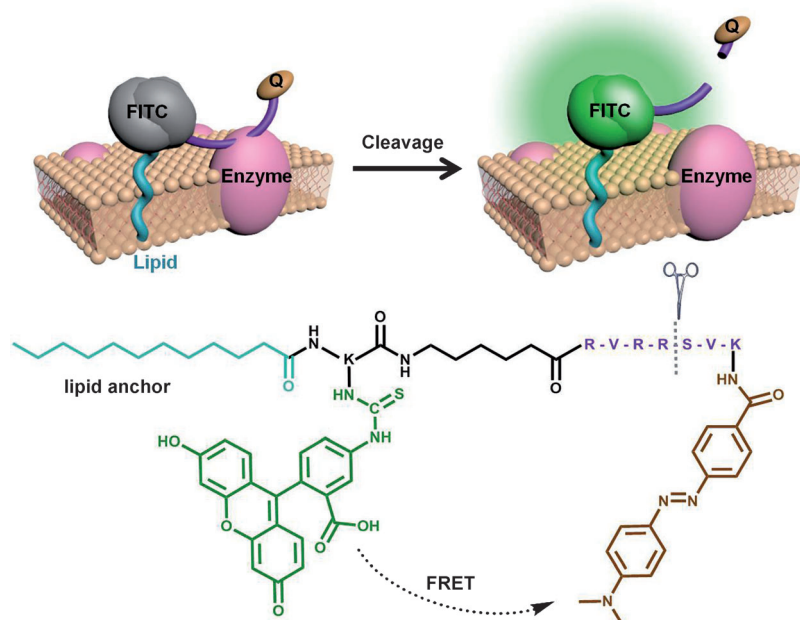
Herein, we present a simple small-molecule-based reporter to effectively visualize furin-like enzyme activities on the cell surface. This well-designed membrane-anchored and furin-responsive probe (MFP) molecule could efficiently confine the probe into the lipid compartments of cell membranes, thereby increasing the effective probe–enzyme interactions. Moreover, this unique reporter also provides a significant opportunity for the real-time visualization of specific extracellular proteolytic enzyme activities in living cells and tissues. The visualization may be achieved through both one-photon and two-photon imaging with minimum autofluorescence and cytotoxic side effects.

Scheme 1 shows the small-molecule reporter prepared in order to image the process of specific furin cleavage on the cell membrane. The consensus peptide sequences (K/R)-(X)_n-(K/R)↓ (where *n* = 0, 2, 4, or 6, K = lysine, and X is any amino acid, respectively),^[3a,10] were chosen as our basic moieties for preferential furin cleavage, which were further integrated with the principles of passive exogenous insertion and Förster

resonance energy transfer (FRET) for the purpose of specific imaging of furin activity.^[11] In our study, the defined peptide sequence RXRR was selected as the main binding pocket, which was subsequently conjugated with small hydrophilic residues (e.g. serine) and hydrophobic residues (e.g. valine) at the C-terminus, respectively, to achieve enhanced enzyme-activatable properties.^[10a] To conduct real-time cell imaging, the enzyme-responsive RVRRSVK peptide was flanked with an activatable FRET pair consisting of fluorescein (FITC) and an effective FITC quencher Dabcyl (4-(dimethylamino-azo)benzene-4-carboxamide), chosen for their spectral overlap. The connection of FITC through a 6-aminohexanoic acid linker was mainly because of its optimal fluorescence quantum yield under physiological conditions and its promising two-photon properties.^[12] More importantly, to immobilize the enzyme-responsive fluorescent probe onto the cell surface,^[13] fatty-acid lipid moieties with different length of carbon chains were carefully screened and were further conjugated with the furin-responsive peptide probe (Scheme S1 and Figure S1 in the Supporting Information). The optimized lipid moiety serves as an efficient targeting vector to anchor the fluorescent probe to the cell surface, in fact mostly to the lipid compartments in the cell membranes, to enhance the specific enzyme interaction.

After preparation of the MFP probe, we first examined the enzyme hydrolysis of the developed MFP probe by measuring the changes in fluorescence emission intensity upon addition of furin in HEPES (4-(2-hydroxyethyl)-1-piperazineethanesulfonic acid) buffer. As shown in Figure 1 A, the MFP probe itself was almost nonfluorescent as a result of efficient FRET quenching. After incubation with

the enzyme for 2 hours, an intense fluorescent enhancement (approximately 12-fold) was detected at a maximum wavelength of $\lambda = 525$ nm, corresponding to emission from the connected FITC. Similar enzyme hydrolysis with a standard inhibitor (Dec-RVKR-cmk) demonstrated a limited fluorescence enhancement after 2 hours incubation time,^[14] suggesting that the specific furin interaction splits the FRET pair by releasing the quencher Dabcyl. Further analysis of the hydrolysis kinetics of the MFP probe by furin in HEPES buffer allowed calculation of the catalytic constant, $k_{\text{cat}} = 2.78 \pm 0.51 \text{ s}^{-1}$, and the Michaelis constant, $K_{\text{m}} = 25.5 \pm 2.1 \text{ }\mu\text{M}$. The enzyme catalytic efficiency ($K_{\text{cat}}/K_{\text{m}}$) for furin was $1.09 \times 10^5 \text{ M}^{-1} \text{ s}^{-1}$. Moreover, the enzyme cleavage effect was examined by HPLC analysis (Figure 1 B). A new peak with a retention time of 10 minutes was observed to increase after incubation with furin for 60 minutes. This new peak was attributable to the enzyme cleavage fragment (S-V-K(Dabcyl)) and was confirmed by LC-MS analysis (Figure 1 C). The retention time of enzymatic reaction mixtures incubated with the furin inhibitor was the same as that of the MFP probe alone, indicating that the developed MFP probe could be specifically



Scheme 1. The structure of the membrane-anchored and furin-responsive probe (MFP) and the corresponding surface-associated cleavage of the probe by furin on the cell membrane. FITC = fluorescein (green structures); Q = Dabcyl quencher molecule (light brown oval). The purple line denotes the cleavable peptide sequence, the blue line denotes the lipid anchor.

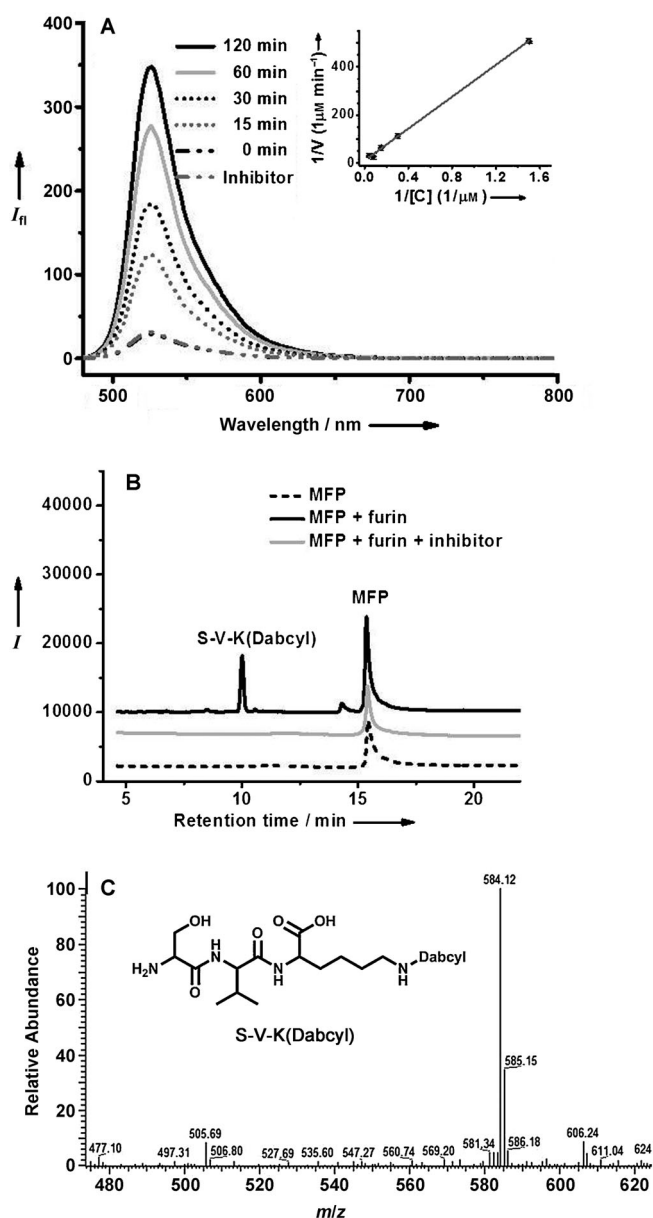


Figure 1. A) Fluorescence enhancement of MFP (6.5 μM ; in HEPES buffer; pH 7.4) when treated with furin with or without inhibitor Dec-RVKR-cmk at different time intervals (0–120 min, $\lambda_{\text{ex}} = 450 \text{ nm}$) at 37°C. Dec-RVKR-cmk (100 μM) was preincubated with the enzyme for 30 minutes prior to the addition of the probe. Inset: the enzyme kinetics of furin (2U) with MFP. B) HPLC traces of MFP alone, MFP with furin, or MFP incubated with the inhibitor before addition of furin for 60 minutes. C) The LC–MS spectrum showing the cleavage product S-V-K(DabcyI).

cleaved by furin. This was consistent with the results obtained through fluorescence measurements.

With the desired enzyme-responsive properties in hand, we tested the applicability of MFP towards furin-dependent cell-surface imaging. In this study, human neuronal glioblastoma U251 cells were selected as our target mainly because of their expression of high levels of furin.^[15] Additionally, furin-deficient Lovo cells (human colon adenocarcinoma cells) were chosen as the negative control.^[16] Typically, U251 and

Lovo cells were incubated with the MFP probe for 15 minutes. As contrast, cell membranes were also tracked with the commercially available CellMask Deep Red dye to monitor the progress of membrane staining.^[8d] As shown in Figure 2, after 15 minutes incubation, strong green fluores-

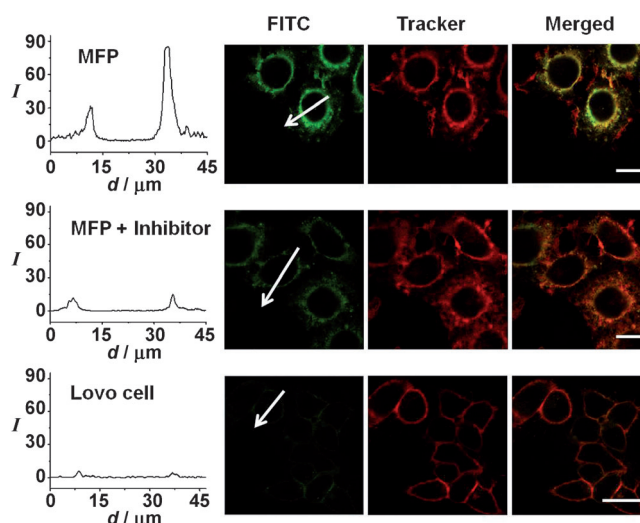


Figure 2. Fluorescence imaging of U251 cells using the MFP probe. Cells were incubated with MFP alone (130 nM) or with MFP and the inhibitor (40 μM) for 15 minutes at 37°C. Standard CellMask Deep Red (2.5 $\mu\text{g mL}^{-1}$) was used to image the membrane. Fluorescence intensity was plotted as a function of distance (d) along with arrows. Lovo cells were incubated with the MFP probe as a control. Scale bar in all images = 20 μm .

cence on the surface of the U251 cells was detected. Moreover, the time-lapse imaging further confirmed the dynamic enzymatic processes on the cell surface, and strong membrane staining could be still detected even after a prolonged incubation period of 1.5 hours (Figure S2 and S3). As the control, no obvious fluorescence was detected in the same cells upon treatment with the furin inhibitor (Dec-RVKR-cmk)^[14] or in the negatively controlled furin-deficient Lovo cells even after incubation with high concentrations of the probe (Figure 2 and S4, Supporting Information). Such promising imaging results demonstrated that the MFP probe could be employed as an effective tracer to report the cell-surface-associated furin activity in living cells.

To further investigate the varying levels of furin expression between U251 and Lovo cells which are responsible for the fluorescence detected on the cell surface, a cell-lysate-based furin assay was conducted by incubation of the MFP probe with cell-lysate samples. In this study, the level of the total protein in the cell lysate was kept constant by using the standard Bradford method.^[17] As shown in Figure 3, a substantially lower fluorescence signal was detected in furin-deficient Lovo cells, whereas a significant fluorescence enhancement was measured in furin-expressed U251 cell lysates over all of the incubation time. Moreover, the furin cleavage in U251 cell lysates was significantly suppressed with the addition of the furin inhibitor, suggesting that the developed

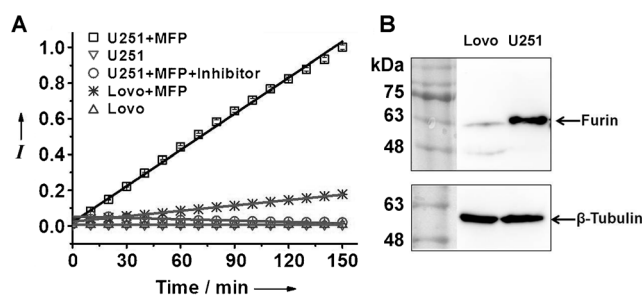


Figure 3. A) Plot showing the change in fluorescence intensity of MFP (10 μM) with time, used to quantify the furin activity in U251 and Lovo cell lysates (10 μg total protein was incubated with MFP at 37 $^{\circ}\text{C}$). The inhibitor Dec-RVKR-cmk (100 μM) was added to U251 cell lysates for 30 minutes prior to addition of the probe. B) Analysis of furin expression by Western blot in U251 and Lovo cells. β -tubulin was included as an internal control.

MFP probe could serve as reliable tracer to quantitatively evaluate specific furin activities in complex environments (Figure 3 A and Figure S5). Similar enzyme cleavage was also confirmed by HPLC and using the standard fluorescent furin substrate Boc-RVRR-AMC (Figures S6 and S7).^[9] To further verify the specific expression level of the furin enzyme in different cells, both cell-lysate samples were analyzed by immunoblotting with anti-furin antibodies. For quantitative analysis, the expression levels of furin were normalized to the internal control of β -tubulin. The chemiluminescence signals in Figure 3B confirmed the highly expressed furin in U251 cells, whereas the same enzyme expression was greatly reduced in Lovo cells.^[15] The different levels of furin expression in U251 and Lovo cells verified by immunoblotting further confirmed that our developed MFP probe could be used to reliably evaluate furin activity in different cells. Finally, we also evaluated the potential cytotoxicity of the MFP probe by using a standard MTT assay (Figure S8). There was no obvious cytotoxicity of the MFP probe to both U251 and Lovo cells even after incubation over a long time, suggesting that the MFP probe could allow real-time visualization of furin activity without affecting physiological processes.

One significant feature of our developed MFP probe was its ability to specifically stain the cell membranes upon its specific reaction with the surface-associated furin enzyme. To confirm if the hydrophobic lipid anchor could facilitate the membrane insertion, a similar fluorescent probe (FP) without fatty acid moiety was also prepared for live-cell imaging (Figure S9). Although enzymatic hydrolysis results clearly indicated that FP could be cleaved by furin in HEPES buffer (Figure S10), the cell-imaging study based on FP alone revealed poor membrane staining when compared to results obtained using MFP (Figure S11). This result clearly showed that the lipid anchor is essential for the localization of the MFP probe on the cell surface. To check whether the chain length in the lipid moiety could affect cell-membrane staining, a similar MFP peptide sequence was used without a Dabcyl quencher connection to conjugate with different fatty acids (e.g. caproic acid, lauric acid and stearic acid, respectively). The as-prepared FITC-peptide-fatty acid conjugates, abbrevi-

ated as C6-F, C12-F, and C18-F, respectively (where C12-F has the same carbon chain as MFP), were incubated with HEK293 cells (human embryonic kidney cells) for different time intervals. As shown in Figure 4 and Figure S12, there was

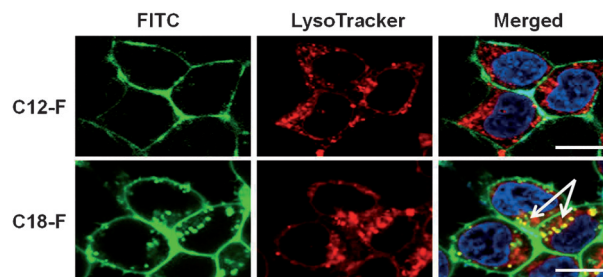


Figure 4. Fluorescence imaging of live HEK293 cells after incubation with FITC-peptide conjugates (C6-F, C12-F, and C18-F; 1 μM) for 2 hours at 37 $^{\circ}\text{C}$. FITC = green fluorescence signal; LysoTracker = red signal; Hoechst dye H33258 (nuclear stain) = blue signal. The arrows show the co-localization of C18-F and LysoTracker (yellow). Scale bar = 15 μm .

almost no fluorescence detected in C6-F incubated HEK293 cells compared to cells treated with C12-F and C18-F. These results confirmed that the increased length of the carbon chain could indeed enhance the immobilization of the probe onto the cell surface. Unlike C12-F, although the C18-F conjugate indeed showed an enhanced tracking ability on the cell membrane, the obvious internalization into the lysosomes would be hard to avoid after prolonged incubation, for example over 2 hours (Figure 4 and Figure S13). Therefore, the MFP probe with a dodecanoyl moiety would be the ideal tracer to specifically localize the probe onto the cell membrane, and thus significantly facilitate long-time trackable visualization of surface-associated furin in living cells. Such long-time membrane anchoring provides the potential to monitor the dynamic processes of cell-surface enzyme activities, which is normally difficult for most established cell-permeable small-molecule probes.

In terms of the two-photon characteristics of FITC (see Supporting Information),^[12,18] we also investigated the possibility to undertake two-photon imaging based on the specific interactions between the developed MFP probe and cell-surface-associated furin enzyme in living cells or tissues. As a proof of concept, U251 cells were incubated with the MFP probe (1.0 μM) at 37 $^{\circ}\text{C}$ for 30 minutes and two-photon imaging was carried out upon excitation of the sample at $\lambda = 800 \text{ nm}$. As shown in Figure 5, strong fluorescent staining on the surface of U251 cells was measured. Similar two-photon imaging was also conducted by incubation of the MFP probe with mouse ear tissues and the images were monitored at depths of approximately 40 μm . The bright fluorescence detected clearly indicated that the developed probe molecule could efficiently monitor furin enzyme activities in living tissues.

In conclusion, the specific localization of our developed MFP probe on the plasma membrane represents a simple and effective small-molecule-based method for the direct visual-

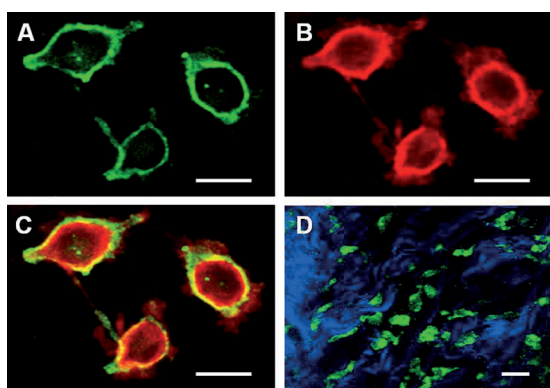


Figure 5. Two-photon imaging in U251 cells and mouse ear tissue after incubation with the MFP probe. Channel: FITC (A), membrane tracker CellMask Deep Red (B), merged images (C). D) MFP signals (green) in tissues and second harmonic generation from collagen (blue). Scale bar = 20 μm .

ization of furin-like enzyme activity on the cell surface. In this study, the carefully optimized lipid moiety in the molecular structure can efficiently facilitate the immobilization of the probe on the extracellular plasma membrane for a relative long time. Upon specific enzyme hydrolysis, a strong fluorescent turn-on effect can be detected, demonstrating the promising real-time imaging of surface-localized furin activities in living cells and tissues using one-photon and two-photon microscopy. This rational design could be also expanded as a reliable and general method to visualize other membrane-associated proteolytic enzymes and their functions and biological roles without the need for invasive procedures. Furthermore, optimization of this type of probe to trace enzyme dynamics and location in specific subcellular organelles will provide a deeper insight into the mechanisms of viral or pathogen invasion, a goal is currently under investigation. More importantly, such a unique MFP probe can also be used to screen potential proteolytic enzyme inhibitors to selectively block furin-dependent cell-surface processing without interfering with normal cell function, which should facilitate the discovery of specific probes or drug molecules towards theranostics of furin-related diseases.

Received: July 14, 2014

Revised: September 26, 2014

Published online: October 27, 2014

Keywords: fluorescence microscopy · FRET · imaging agents · proteolytic enzymes · two-photon imaging

- [1] a) M. S. Brown, J. Ye, R. B. Rawson, J. L. Goldstein, *Cell* **2000**, *100*, 391; b) A. Weihofen, B. Martoglio, *Trends Cell Biol.* **2003**, *13*, 71; c) S. Urban, M. Freeman, *Curr. Opin. Genet. Dev.* **2002**, *12*, 512.
- [2] a) A. J. Barrett, J. F. Woessner, N. D. Rawlings, *Handbook of proteolytic enzymes, Vol. 1*, Elsevier, Amsterdam, **2004**; b) M. S. Wolfe, *Chem. Rev.* **2009**, *109*, 1599; c) T. Jiang, E. S. Olson, Q. T. Nguyen, M. Roy, P. A. Jennings, R. Y. Tsien, *Proc. Natl. Acad. Sci. USA* **2004**, *101*, 17867.

- [3] a) G. Thomas, *Nat. Rev. Mol. Cell Biol.* **2002**, *3*, 753; b) N. G. Seidah, A. Prat, *Nat. Rev. Drug Discovery* **2012**, *11*, 367.
- [4] a) P. Stawowy, C. Margeta, H. Kallisch, N. G. Seidah, M. Chrétien, E. Fleck, K. Graf, *Cardiovasc. Res.* **2004**, *63*, 87; b) M. Roomi, J. Monterrey, T. Kalinovsky, M. Rath, A. Niedzwiecki, *Oncol. Rep.* **2009**, *21*, 1323.
- [5] E. Hwang, S. Kim, J. Sohn, J. Lee, Y. Kim, Y. Kim, I. Mook-Jung, *Biochem. Biophys. Res. Commun.* **2006**, *349*, 654.
- [6] a) S. A. Shiryaev, A. G. Remacle, B. I. Ratnikov, N. A. Nelson, A. Y. Savinov, G. Wei, M. Bottini, M. F. Rega, A. Parent, R. Desjardins, *J. Biol. Chem.* **2007**, *282*, 20847; b) T. Matsuzawa, A. Fukui, T. Kashimoto, K. Nagao, K. Oka, M. Miyake, Y. Horiguchi, *J. Biol. Chem.* **2004**, *279*, 2866; c) T. Komiyama, J. M. Coppola, M. J. Larsen, M. E. V. Dort, B. D. Ross, R. Day, A. Rehemtulla, R. S. Fuller, *J. Biol. Chem.* **2009**, *284*, 15729.
- [7] a) D. Mesnard, D. B. Constam, *J. Cell Biol.* **2010**, *191*, 129; b) K. Gawlik, A. G. Remacle, S. A. Shiryaev, V. S. Golubkov, M. Ouyang, Y. Wang, A. Y. Strongin, *PLoS One* **2010**, *5*, e11305; c) J. P. Hobson, S. Liu, B. Rønø, S. H. Leppla, T. H. Bugge, *Nat. Methods* **2006**, *3*, 259; d) Y. Yano, K. Matsuzaki, *Biochim. Biophys. Acta Biomembr.* **2009**, *1788*, 2124.
- [8] a) D. S. Folk, J. C. Torosian, S. Hwang, D. G. McCafferty, K. J. Franz, *Angew. Chem. Int. Ed.* **2012**, *51*, 10795; *Angew. Chem.* **2012**, *124*, 10953; b) M. H. Lee, H. M. Jeon, J. H. Han, N. Park, C. Kang, J. L. Sessler, J. S. Kim, *J. Am. Chem. Soc.* **2014**, *136*, 8430; c) S. Mizukami, Y. Hori, K. Kikuchi, *Acc. Chem. Res.* **2014**, *47*, 247; d) L. Li, X. Shen, Q. Xu, S. Yao, *Angew. Chem. Int. Ed.* **2013**, *52*, 424; *Angew. Chem.* **2013**, *125*, 442; e) T. Kowada, J. Kikuta, A. Kubo, M. Ishii, H. Maeda, S. Mizukami, K. Kikuchi, *J. Am. Chem. Soc.* **2011**, *133*, 17772; f) J. Lovell, T. Liu, J. Chen, G. Zheng, *Chem. Rev.* **2010**, *110*, 2839; g) L. E. Edgington, M. Verdoes, M. Bogyo, *Curr. Opin. Chem. Biol.* **2011**, *15*, 798; h) E. A. Lemke, C. Schultz, *Nat. Chem. Biol.* **2011**, *7*, 480; i) B. E. Cravatt, A. T. Wright, J. W. Kozarich, *Annu. Rev. Biochem.* **2008**, *77*, 383; j) L. Bu, X. Ma, Y. Tu, B. Shen, Z. Cheng, *Curr. Pharm. Biotechnol.* **2014**, *14*, 723.
- [9] a) S. Molloy, P. Bresnahan, S. H. Leppla, K. Klimpel, G. Thomas, *J. Biol. Chem.* **1992**, *267*, 16396; b) S. M. Cork, B. Kaur, N. S. Devi, L. Cooper, J. H. Saltz, E. M. Sandberg, S. Kaluz, E. G. Van Meir, *Oncogene* **2012**, *31*, 5144.
- [10] a) N. C. Rockwell, D. J. Krysan, T. Komiyama, R. S. Fuller, *Chem. Rev.* **2002**, *102*, 4525; b) A. Dragulescu-Andrasi, S.-R. Kothapalli, G. A. Tikhomirov, J. Rao, S. S. Gambhir, *J. Am. Chem. Soc.* **2013**, *135*, 11015; c) A. Dragulescu-Andrasi, G. Liang, J. Rao, *Bioconjugate Chem.* **2010**, *20*, 1660.
- [11] a) D. Rabuka, M. B. Forstner, J. T. Groves, C. R. Bertozzi, *J. Am. Chem. Soc.* **2008**, *130*, 5947; b) H. Kim, B. Kim, H. Choo, Y. Ko, S. Jeon, C. Kim, T. Joo, B. Cho, *ChemBioChem* **2008**, *9*, 2830; c) K. E. Sapsford, L. Berti, I. L. Medintz, *Angew. Chem. Int. Ed.* **2006**, *45*, 4562; *Angew. Chem.* **2006**, *118*, 4676.
- [12] K. Samuelsson, C. Simonsson, C. A. Jonsson, G. Westman, M. B. Ericson, A. T. Karlberg, *Contact Dermatitis* **2009**, *61*, 91.
- [13] a) A. Cobos-Correa, J. B. Trojanek, S. Diemer, M. A. Mall, C. Schultz, *Nat. Chem. Biol.* **2009**, *5*, 628; b) S. Gehrig, M. A. Mall, C. Schultz, *Angew. Chem. Int. Ed.* **2012**, *51*, 6258; *Angew. Chem.* **2012**, *124*, 6363; c) L. Rajendran, A. Schneider, G. Schlechttingen, S. Weidlich, J. Ries, T. Braxmeier, P. Schwill, J. B. Schulz, C. Schroeder, M. Simons, G. Jennings, H. Knolker, K. Simons, *Science* **2008**, *320*, 520; d) Y. Hu, D. Vats, M. Vizovisek, L. Kramer, C. Germanier, K. U. Wendt, M. Rudin, B. Turk, O. Plettenburg, C. Schultz, *Angew. Chem. Int. Ed.* **2014**, *53*, 7669; *Angew. Chem.* **2014**, *126*, 7802; e) D. Lingwood, K. Simons, *Science* **2010**, *327*, 46.
- [14] S. Henrich, A. Cameron, G. P. Bourenkov, R. Kiefersauer, R. Huber, I. Lindberg, W. Bode, M. Than, *Nat. Struct. Mol. Biol.* **2003**, *10*, 520.

- [15] a) A. G. Remacle, A. V. Chekanov, V. S. Golubkov, A. Y. Savinov, D. V. Rozanov, A. Y. Strongin, *J. Biol. Chem.* **2006**, *281*, 16897; b) S. A. Shiryaev, A. V. Chernov, V. S. Golubkov, E. R. Thomsen, E. Chudin, M. S. Chee, I. A. Kozlov, A. Y. Strongin, P. Cieplak, *Plos One* **2013**, *8*, e54290.
- [16] S. Takahashi, T. Nakagawa, K. Kasai, T. Banno, S. J. Duguay, W. J. Van de Ven, K. Murakami, K. Nakayama, *J. Biol. Chem.* **1995**, *270*, 26565.
- [17] a) G. L. Bourne, D. J. Grainger, *J. Immunol. Methods* **2011**, *364*, 101; b) N. J. Kruger, in *Basic Protein and Peptide Protocols*, Springer, Heidelberg, **1994**, p. 9.
- [18] a) M. Pawlicki, H. A. Collins, R. G. Denning, H. L. Anderson, *Angew. Chem. Int. Ed.* **2009**, *48*, 3244; *Angew. Chem.* **2009**, *121*, 3292; b) G. Egawa, S. Nakamizo, Y. Natsuaki, H. Doi, Y. Miyachi, K. Kabashima, *Sci. Rep.* **2013**, *3*, 1.
-